Bulletin of the *Transilvania* University of Braşov • Vol. 13 (62) No. 2 - 2020
Series I: Engineering Sciences
https://doi.org/10.31926/but.ens.2020.13.62.1.7

SEM AND XRD CHARACTERISATION OF FUSION LINES OBTAINED ON AUSTEMPERED DUCTILE IRON BY LASER BEAM WELDING WITHOUT PREHEATING

I.C. MON[1] M.H. TIEREAN[1] L.S. BALTES[1]

Abstract: *This study highlights the weldability of austempered ductile iron (ADI) using laser welding. SEM, EDS and XRD analysis were performed on fusion lines, heat affected zone (HAZ) and melted zone (MZ). Welding speed (Ws) and laser power (P) were varied. The heat affected zone is composed of graphite, perlite and martensite; the melted and solidified zone contains graphite, ferrite and cementite. XRD results are in accordance with SEM micrographs.*

Key words: *Austempered Ductile Iron, laser, welding, SEM, EDS, XRD.*

1. Introduction

Austempered ductile iron (ADI) is an alternative material for traditional forging and casting steel, due to the good mechanical properties [1-3] and applicability in manufacturing of engine valves, gears, crankshaft etc. [15]. Meneghetti, G. et al. [4] analyzed from metallographic and microhardness point of view the fatigue strength of EN-JS-1050 ADI to S355J2 steel dissimilar arc-welded joints. The tests showed the superior performance of ADI to steel than those suggested by International Standards and Recommendation for the welded joints and recommend to develop this subject for future research. Soriano, C. et al. [12] have shown the efficiency of laser surface hardening in improving the mechanical properties of ADI. X-ray diffraction scan reveal the values of residual stresses in agreement with microhardness (650-800 HV) and microstructural variation (coarse martensite with retained austenite in the treated area). Similar results of surface hardening (770 HV) using low laser power intensity were obtained on ADI by Zammit et al. [13]. SEM and XRD analysis showed a structure composed of martensite with unaltered graphite nodules. Research has also shown that for ADI, laser surface hardening parameters must be carefully controlled. Also according to Zammit et al [14] laser hardening improves the rolling contact fatigue resistance of ADI samples, according to SEM micrographs.

The goal of the present paper is the testing of laser beam weldability of austempered ductile iron without preheating, using SEM, EDS and XRD tests. This paper is a continuation of Mon et al. [5-8] research, especially the previous paper [9].

[1] Dept. of Materials Engineering and Welding, *Transilvania* University of Braşov, Romania.

2. Materials and Methods

The material used in the experimental research to perform laser beam welding tests without additive material was ADI, Grade 1050/750/07 (ASTM A897M-03), provided by the Central Metallurgical Research and Development Institute Egypt. Mechanical properties, the technology of application the laser welding regimes and optical microscopy results were presented in the previous paper [9]. Chemical composition of the samples was performed using the JOEL scanning electron microscope (SEM), JSM-6610LA model, with EDS spectrometer, from the Bourgogne University, Carnot Interdisciplinary Laboratory - Laser and Materials Processing. The identification of the various crystalline compounds was performed using a PANALYTICAL X-ray diffractometer (XRD), X 'PERT PRO model, with Bragg-Bretano geometry (2θ), from the same university.

3. Results and Discussions

Figure 1 presents the SEM micrographs of the melted zone (MZ) and heat affected zone (HAZ) after obtaining the fusion lines on the ADI samples, without preheating, following the parameters *P* = 5 [kW] and *Ws* = 0.6 [m / min].

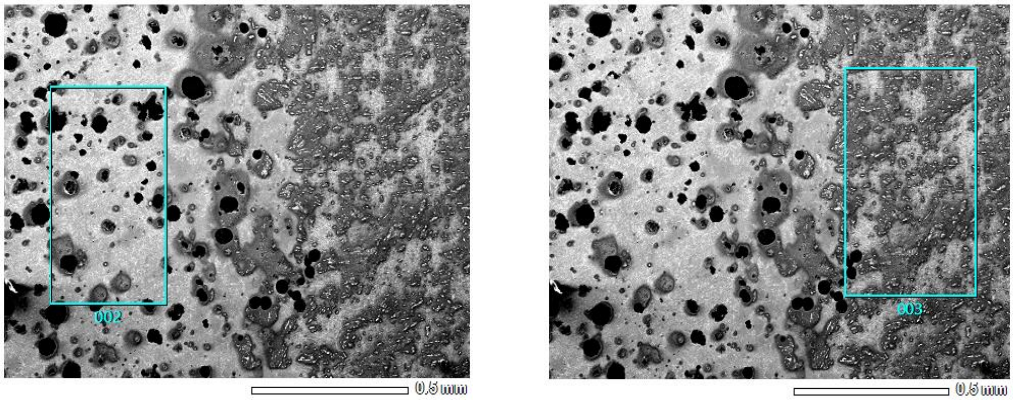

Fig. 1. *SEM micrograph of HAZ (002 area) and MZ (003 area), magnification 85X*

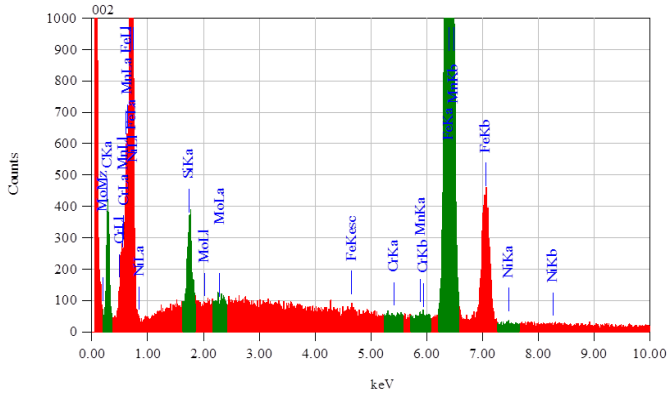

Fig. 2. *Energy dispersive spectroscopy (EDS) of HAZ (002 specific area from Figure 1)*

The distributions of the main alloying elements in specific areas 002 and 003 are presented in Figures 2 and 3. In the heat affected zone the carbon content is higher (Figure 2).

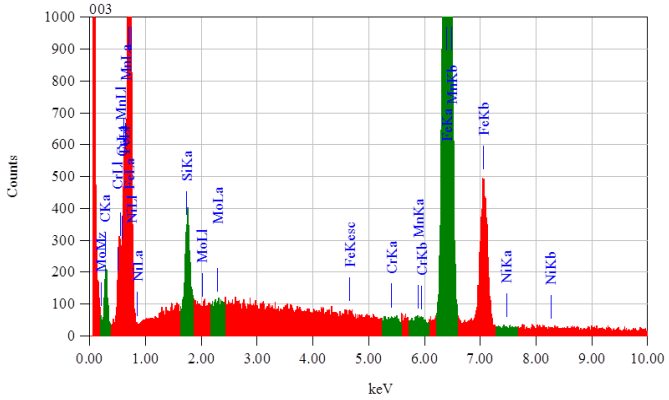

Fig. 3. *Energy dispersive spectroscopy (EDS) of MZ (003 specific area from Figure 1)*

Figure 4 presents the SEM micrographs of the melted zone (MZ) and heat affected zone (HAZ) after obtaining the fusion lines on the ADI samples, without preheating, following the parameters *P* = 4.5 [kW] and *Ws* = 0.5 [m / min].

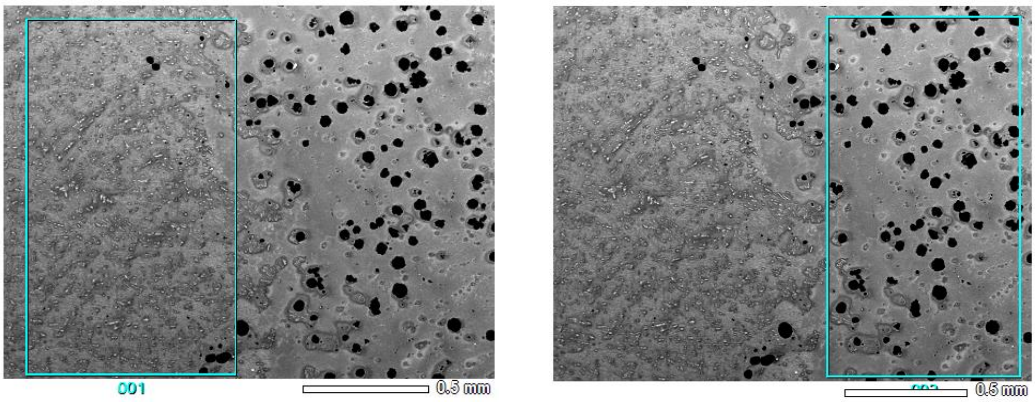

Fig. 4. *SEM micrograph of HAZ (002 area) and MZ (001 area), magnification 65X*

The distribution of the main alloying elements in the specific area 001 and 002 is highlighted in Figures 5 and 6, images obtained in the X-ray dispersive field. In the heat affected zone the carbon content is higher (Figure 6), the measuring area containing graphite nodules.

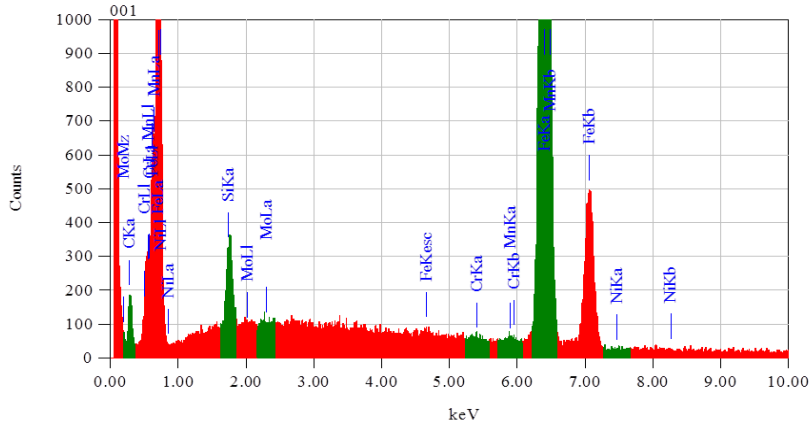

Fig. 5. *Energy dispersive spectroscopy (EDS) of MZ (001 specific area from Figure 4)*

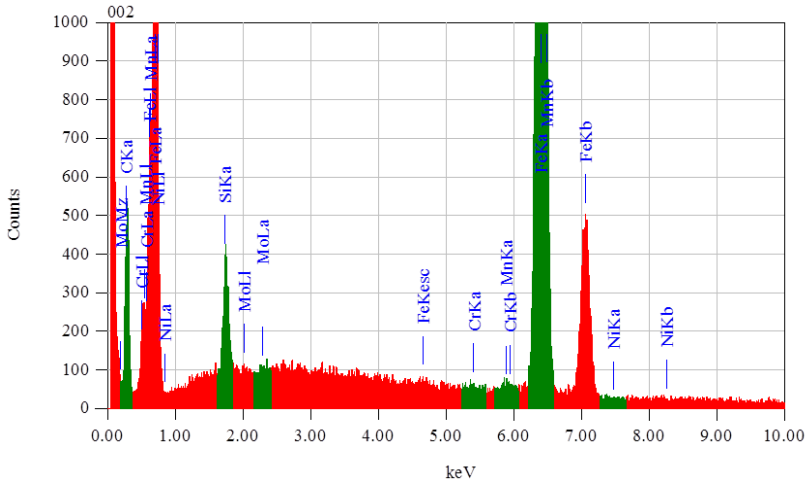

Fig. 6. *Energy dispersive spectroscopy (EDS) of HAZ (002 specific area from Figure 4)*

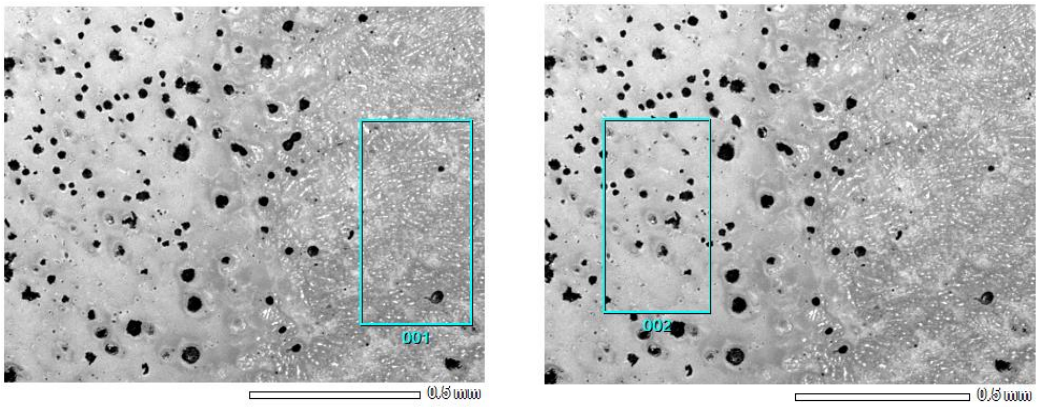

Fig. 7. *SEM micrograph of HAZ (002 area) and MZ (001 area), magnification 90X*

Figure 7 presents the SEM micrographs of the melted zone (MZ) and heat affected zone (HAZ) after obtaining the fusion lines on the ADI samples, without preheating, following the parameters *P* = 4.5 [kW] and *Ws* = 0.6 [m / min].

The distribution of the main alloying elements in specific areas 001 and 002 is presented in Figures 8 and 9.

The specific area 002 of the heat affected zone containing graphite nodules, has a higher carbon content than in specific area 001.

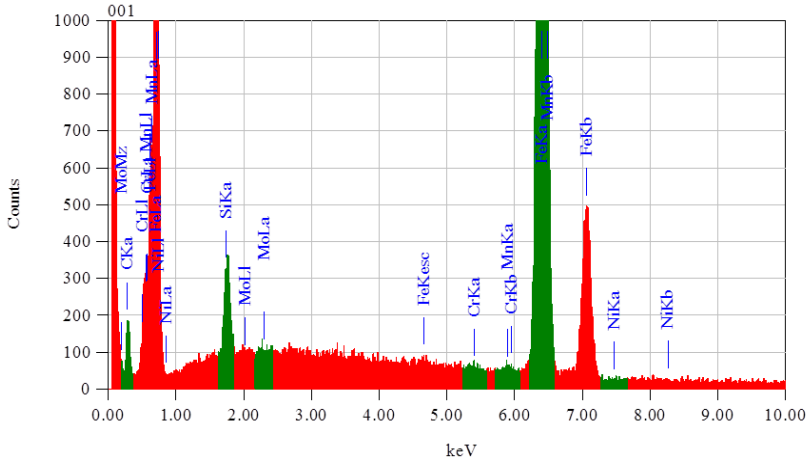

Fig. 8. *Energy dispersive spectroscopy (EDS) of MZ (001 specific area from Figure 7)*

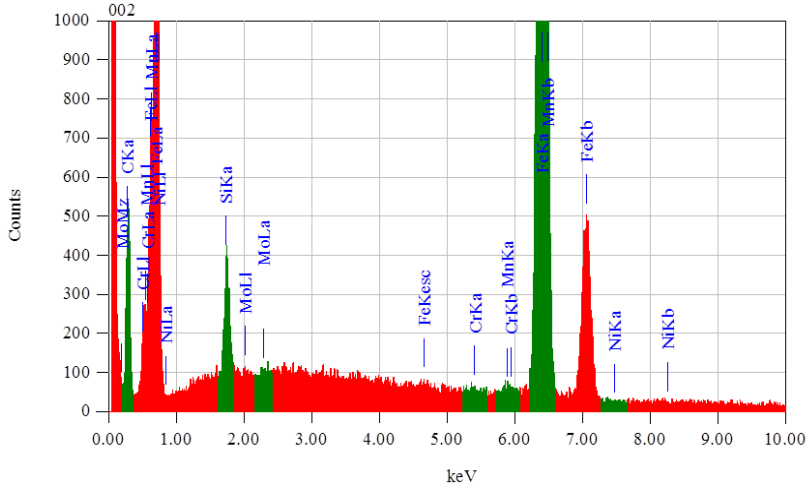

Fig. 9. *Energy dispersive spectroscopy (EDS) of HAZ (002 specific area from Figure 7)*

Maintaining a constant welding speed of 0.6 m/min and increasing the laser power from 4.5 kW to 5 kW, was found an increasing of the manganese content in both zones (from 2.08% to 2.25% in HAZ and from 2.19% to 2.63% in MZ). Increasing the laser power silicon content has only a small variation (decreasing from 1.69% to 1.66% in HAZ and increasing from 1.6% to 1.77% in MZ).

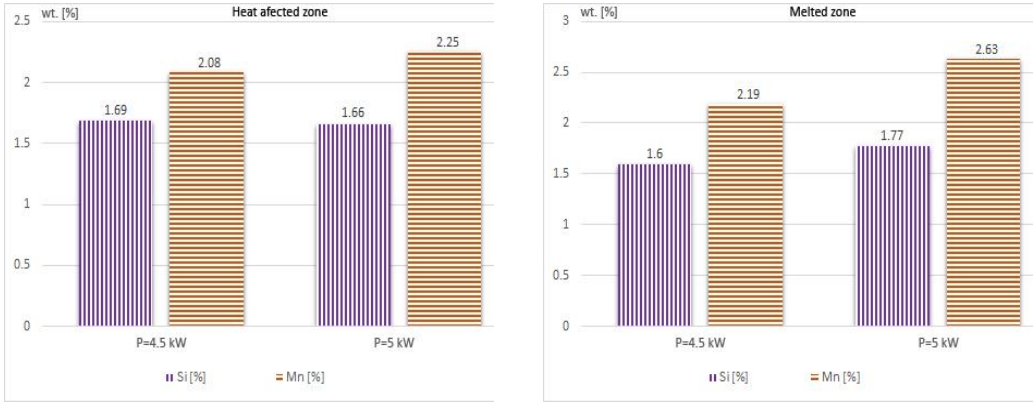

Fig. 10. *Variation of chemical composition with power (P) for Ws = 0.6 m/min on ADI samples without preheating: a) HAZ, b) MZ*

The same trend is highlighted in the case of keeping the power constant at *P* = 4.5 kW and increasing the welding speed from 0.5 m/min to 0.6 m/min. Figure 11 reveals the increasing of silicon content from 1.49% to 1.69% in HAZ and from 1.4% to 1.6% in MZ. In HAZ manganese increase from 1.99% to 2.08%, but in MZ decrease from 2.43% to 2.19%.

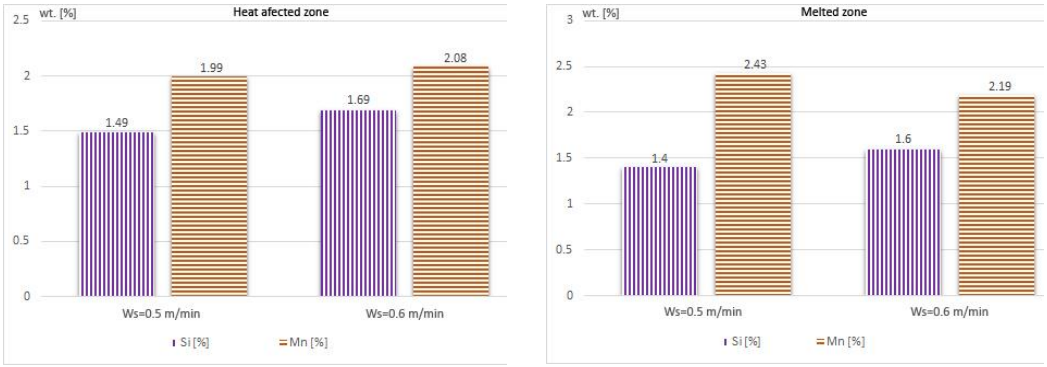

Fig. 11. *Variation of the chemical composition with welding speed (Ws) for P = 4.5 kW on ADI specimens without preheating: a) HAZ, b) MZ*

Figure 12 presents the X-ray diffraction (XRD) diffractogram obtained after the comparison between the fusion lines on the ADI samples with and without preheating with the parameters: *P* = 5.5 kW and *Ws* = 0.8 m / min (without preheating), *P* = 4.5 kW and *Ws* = 0.6 m / min (with preheating).

The overlapping of the diagrams with and without preheating are observed. It had to remarque the peaks of graphite (Carbon; P63/mmc), ferrite (Iron; Im-3m), cementite (Iron Carbon; Fm-3m), martensite (I4/mmm).

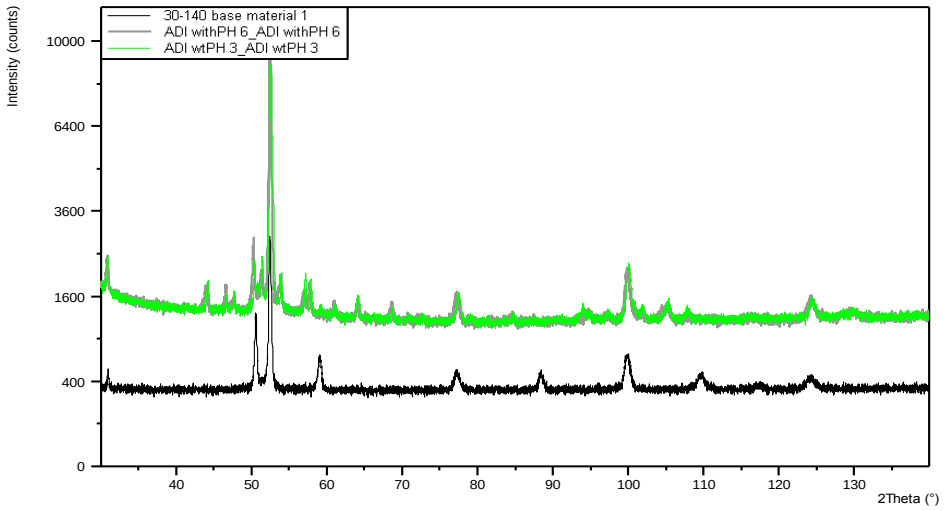

Fig. 12. *Comparison between fusion lines on ADI samples with / without preheating with parameters: P = 5.5 [kW] and Ws = 0.8 [m / min] (without preheating), P = 4.5 [kW] and Ws = 0.6 [m/min] (with preheating) and ADI base material*

4. Conclusions

SEM characterisation leads to the same structure find in [9]: the heat affected zone is composed of graphite, perlite and martensite; the melted and solidified zone contains graphite, ferrite and cementite. There were observed more graphite nodules in HAZ than in MZ, where there were replaced by cementite. XRD of fusion lines on ADI samples reveals similar results. Due to presence of cementite and martensite in melted zone, the laser welding of ADI without preheating is not recommended.

In all EDS analysed cases the manganese content is greater than silicon content. The increasing of the Si content determines the decreasing of the carbon solubility in austenite while the high manganese content favours the appearance of martensite in heat affected zones as mentioned in [10, 11]. This increasing of Mn content leads the hardening of HAZ and MZ, causing to the non-recommendation of laser welding of ADI.

Acknowledgements

We would like to thank professor Adel Nofal from Central Metallurgical Research and Development Institute Egypt, for providing ADI samples. We also thank to professor Eugen Cicala and the staff of the research centre from University of Bourgogne, Carnot Interdisciplinary Laboratory of Bourgogne (ICB)-Laser and Materials Processing, for their support.

References

1. Agüera, F.R., Ansaldi, A., Reynoso, A., Fierro, V., Villar, N.A., Aquino, D., Ayllón, E.S.: *Analisis de soldadura de fundiciones ADI con electrodos de Fe-Ni*, CONAMET/SAM 2008.

2. Bejinariu, C., Munteanu, C., Florea, C.D., Istrate, B., Cimpoesu, N., Alexandru, A., Sandu, A.V.: *Electro-chemical Corrosion of a Cast Iron Protected with a Al_2O_3 Ceramic Layer*. In: Revista de Chimie **69** (2018) No. 12, p. 3586-3589.
3. Bendaoud, I., Mattei, S., Cicala, E., Tomashchuk, I., Andrzejewski, H., Sallamand, P., Mathieu, A., Bouchaud, F.: *The Numerical Simulation of Heat Transfers During A Hybrid Laser- MIG Welding Using Equivalent Heat Source Approach*. In: Optics & Laser Technology **56** (2014), p. 334-342.
4. Meneghetti, G., Campagnolo, A., Berto, D., Pullin, E., Masaggia, S.: *Fatigue Properties of Austempered Ductile Iron-To-Steel Dissimilar Arc-Welded Joints*. In: Procedia Structural Integrity **24** (2019), p. 190-203, DOI: 10.1016/j.prostr.2020.02.016.
5. Mon, I.C., Tierean, M.H.: *A Review on Tests of Austempered Ductile Iron Welding*. In: Bulletin of the *Transilvania* University of Brașov, (2015) Vol. 8 (57), Series I, p. 59-66.
6. Mon, I.C., Tierean, M.H., Cicala, E., Pilloz, M., Tomashchuk, I., Sallamand, P.: *Characterization of Fusion Lines Obtained with Laser Welding On Ductile Iron Plates*. In: Solid State Phenomena **254** (2016), p. 33-42.
7. Mon, I.C., Tierean, M.H., Nofal, A.: *Research on GTAW/SMAW Weldability of ADI/DI using Electrodes ENi-Cl and ENiFe-Cl-A*. In: Advanced Materials Research **1128** (2015), Trans Tech Publications, Switzerland, p. 242-253.
8. Mon, I.C.: *Cercetări privind sudabilitatea fontelor ADI* (*Researches Concerning the Weldability of Austempered Ductile Iron*). In: Ph.D. Thesis, *Transilvania* University of Braşov, Braşov, Romania, 2017.
9. Mon, I.C., Tierean, M.H., Baltes, L.S.: *Optical Microscopy Characterisation of Fusion Lines Obtained on Austempered Ductile Iron by Laser Beam Welding Without Preheating*. In: Bulletin of the Transilvania University of Braşov, Series I: Engineering Sciences, Vol. 13 (62) No. 1 - 2020, p. 19-26, DOI: 10.31926/but.ens.2020.13.62.1.3.
10. Nofal, A., Amin, M., Sayed, M.: *Weldability of ADI and the Applied NDT Methods*. In: South African Metal Casting Conference 2017, www.metalcastingconference.co.za.
11. Riposan, I., Sofroni, L., Chişamera, M.: *Fonta bainitică* (*Bainite Cast Iron*). Editura Tehnică, Bucureşti, 1988.
12. Soriano, C., Leunda, J., Lambarri, J., García Navas, V., Sanz, C.: *Effect of Laser Surface Hardening on the Microstructure, Hardness and Residual Stresses of Austempered Ductile Iron Grades*. In: Applied Surface Science257 (2011), p. 7101-7106, DOI: 10.1016/j.apsusc.2011.03.059.
13. Zammit, A., Abela, S., Betts, J.C., Grech, M.: *Discrete Laser Spot Hardening of Austempered Ductile Iron*. In: Surface and Coatings Technology **331(15)** (2017), p. 143-152, DOI: 10.1016/j.surfcoat.2017.10.054.
14. Zammit, A., Abela, S., Betts, J.C., Michalczewski, R., Kalbarczyk, M., Grech, M.: *Scuffing and Rolling Contact Fatigue Resistance of Discrete Laser Spot Hardened Austempered Ductile Iron*. In: Wear **422-423** (2019), p. 100-107, DOI: 10.1016/j.wear.2019.01.061.
15. Wang, B., Barber, G.C., Qiu, F., Zou, Q., Yang, H.: *A Review: Phase Transformation and Wear Mechanisms of Single-Step and Dual-Step Austempered Ductile Irons*. In: Journal of Materials Research and Technology **9(1)** (2020), p. 1054-1069, DOI: 10.1016/j.jmrt.2019.10.074.